Time of emergence for altimetry-based significant wave height changes in the North Atlantic

Antoine Hochet[1], Guillaume Dodet[1], Florian Sévellec[1], Marie-Noëlle Bouin[1],

Anindita Patra[1], Fabrice Ardhuin[1]

[1]Laboratoire d'Océanographie Physique et Spatiale, Univ Brest CNRS IRD Ifremer, Brest, France

Contents of this file

Introduction

In this supporting information, we first compare the North Atlantic(NA) JFM H_s variability in different global wave reanalysis and hindcasts (Text S1, Fig. S1 and S2). Then, we assess the statistical reconstruction of H_s from the Sea level Pressure (Text S2, Fig. S3). In Text S3 and Fig. S4, we assess the number of members required to decompose the NAO index trend.

Then (Text S4, Figure S5), we compute the spatial correlation between the trend computed on the North Atlantic reconstructed H_s ensemble mean and the trend computed on each individual members as a function of the duration of the trend (starting from 1993).

Finally, in table T1, H_s in the three regions of interest is decomposed into the most common modes of atmospheric inter-annual to decadal variability over the North Atlantic.

Text S1. The purpose of this section is to compare the JFM H_s variations in the North Atlantic as given by various datasets. We first compare the JFM H_s trends in these datasets for the 1980-2014 period (Fig. S1), which corresponds to the longest available period of time for the datasets under consideration here. Following the classification used in (Erikson et al., 2022), these datasets are either global ocean wave reanalysis coupled and with wave data assimilation: ERA5 (Hersbach et al., 2020); global ocean wave hindcasts uncoupled without wave data assimilation: with sea-ice forcing: IORAS(Sharmar et al., 2021), NOC(Bricheno & Wolf, 2018), GOW1(Reguero et al., 2012); CFSR-driven wave hindcasts with sea-ice forcing CSIRO-CAWR (Smith et al., 2021) IFREMER-CFSR Stopa, Ardhuin, Babanin, and Zieger (2016); global wave hindcast without sea-ice forcing: JRC-ERAIMentaschi, Vousdoukas, Voukouvalas, Dosio, and Feyen (2017), JRC-CFSR Mentaschi et al. (2017). The detailed description of the H_s datasets used here can be

found in (Erikson et al., 2022). The comparison of the 1980-2014 JFM H_s trends in the NA for these 8 different datasets reveals that the patterns are overall similar with negative values in the North East and positive values at lower latitudes in the western part of the basin. The largest differences are found for the Ifremer and NOC dataset. To further assess the differences between these datasets, we also show the NA average of the JFM time series (Fig. S2). The mean of the individual time correlation between ERA5 and the 7 datasets is 0.76 and goes up to 0.84 if the NOC dataset is removed, suggesting that the agreement between the different datasets for the JFM H_s in the North Atlantic is high.

Text S2. To assess the statistical model given by equation (6), we first compute the β_i coefficients (i.e. the projection of JFM H_s on the JFM SLP principal components) using the 1950-1992 period. Then, the time correlation between the ERA-5 JFM H_s and the reconstructed JFM H_s obtained using Eq. (6) and ERA-5 JFM SLP over the 1993-2018 period are computed. Using these two disjoint periods of time insures that the reconstruction is independent from the calibration. We find that the best results are obtained when 25 EOFs of SLP are used. In Figure S3, the correlation is high (> 0.75) almost everywhere and has a mean of 0.72 when non-significant values are excluded. Non significant correlations are mostly found at low latitudes and close to the western boundary of the basin. In the following section, we use the full period of ERA-5 (1950-2018) to train the statistical model which will be used to derive H_s from a large ensemble of climate simulations.

Text S3.

To assess the number of members needed to decompose the forced and internal signal we investigate the number of members required to decompose the NAO index trend into forced and internal components. The NAO index $\mathrm{INDEX_{NAO}}$ is obtained by regressing the first EOF of SLP, computed for year 1993 over the CESM2 LENS2 ensemble dimension, over the SLP anomaly:

$$\mathrm{INDEX_{NAO}}(ens,t) = \int_S \mathrm{EOF}^0(x,y)\mathrm{SLPA}(x,y,t,ens)\mathrm{d}x\mathrm{d}y \quad (1)$$

where EOF^0 is the normalized first EOF of SLP computed over the north Atlantic at year 1993 over the ensemble dimension that corresponds to the NAO, and where *ens* is the ensemble member index. Then the NAO trends are computed for all members, starting in 1993 and ending between 2018 to 2100 i.e. a duration between 25 and 107 years. The normalized ensemble mean trend of the NAO index is shown in black (Fig. S4) and is always positive. We also compute the standard deviation of the trend as a function of its duration by randomly choosing 5, 10, 30 or 50 members among the 80 available members and by performing 10 000 realisations for each case. When the ensemble mean trend of the NAO index is smaller than 1.64 times the standard deviation of the X members sub-ensemble (where X=5, 10, 30 or 50), it means that there is only a 5% chance that computing the trends by averaging over the X members gives a different trend sign than with the 80 members ensemble mean. In other words, if the 1.64 times standard deviation is smaller than the mean, then the forced component of the NAO index trend can extracted with only X members. Figure S5 shows that the number of members needed to decompose the signal depends on the trend duration. With longer trend duration less members are required. For satellite-era duration (i.e. around 30 years) more than 50 members are

needed to decompose the NAO trend. However for longer trends, for instance 70 years, only 5 members are required.

Text S4.

Figure S5 shows the spatial correlation between the North Atlantic reconstructed H_s ensemble mean trend and the individual H_s trend in each member for different period of times all starting in 1993 i.e.:

$$\mathrm{corr}_{2D}(A,B) = \frac{\sum_{k,l}\left(A_{k,l} - \langle A\rangle\right)\left(B_{k,l} - \langle B\rangle\right)}{\left(\sum_{k,l}\left(A_{k,l} - \langle A\rangle\right)^2\right)^{\frac{1}{2}}\left(\sum_{k,l}\left(B_{k,l} - \langle B\rangle\right)^2\right)^{\frac{1}{2}}} \tag{2}$$

where $A = (A_{k,l})$ and $B = (B_{k,l})$ are the 2D trends with (k,l) longitudes and latitudes indices, and where $\langle A\rangle, \langle B\rangle$ are the spatial average of A and B. As expected, the ensemble mean of the spatial correlation between the ensemble mean reconstructed H_s trend and the reconstructed H_s trend computed for each member increases when the time period is longer. Around 2020, the spatial correlation is mostly contained between -0.25 and 0.7, with a mean value close to 0.25. It indicates that the reconstructed H_s trend in some members is completely uncorrelated with the trend from the ensemble mean. The blue shading shows members with 95% of the largest correlation values and the blue line is the separation between the 5% smallest values and 95% largest. The 5% correlation value becomes larger than 0.5 around 2060 which means by this date, only 5% of the ensemble members have correlations smaller than 0.5.

Figure S1

Comparison of the 1980-2014 JFM H_s trends in the North Atlantic for 8 different datasets.

Figure S2

Time series of the NA average JFM H_s anomalies obtained from 8 different datasets. The ERA-5 time serie, used in this article, is shown in black.

Figure S3

Time correlation between the 1993-2018 reconstructed H_s and ERA-5 H_s. Only 5% significant values are shown. The three specifically studied locations are indicated with orange stars.

Figure S4

Ensemble mean trend of the North Atlantic Oscillation index (black line) and 1.64 standard deviation of the same index (dashed) computed using 5, 10, 30 and 50 members of the CESM2 LENS2 ensemble. The trends are given as a function of the duration since 1993 (in year). The date (or duration) for which the 1.64 standard deviation curve for X members (X=5, 10, 30 or 50) intersects the ensemble mean (black) curve can be interpreted as the date of emergence of the forced signal in the X-member sub-ensemble. The forced NAO trend can be extracted with only 5 members if we consider trends longer than 70 years, whereas more than 50 members are required for trends shorter than 30 years.

Figure S5

Spatial correlation between the H_s trend computed on the ensemble mean and the trend computed on each individual members between 1993 (the CCI v1 dataset start) and the end date shown as the x-coordinate. The black line is the mean of the spatial correlation between the ensemble mean trend and each individual member trend, the orange lines show the values that are within one standard deviation from the mean, blue

shading shows members with 95% of the largest correlation values and the blue line is the separation between the 5% smallest values and 95% largest.

Table S1.

In order to link H_s variability in the three regions of interest with well documented climate indices that are known to influence atmospheric variability in the NA, we compute the correlations between H_s in each location and the following indices: the North Atlantic Oscillation (NAO), the Eastern Atlantic pattern (EA), the Scandinavian index (SCAN), The Eastern Atlantic Western Russia index (EAWR), the Pacific North America index (PNA), the NINO3.4 index (ENSO) which is one of the indices used to characterize the El niño Southern Oscillation and the Tropical Northern Hemisphere index (TNH) (see Table 1 of the supporting information). The climate indices are selected for there known influence on the winter North Atlantic H_s climate (see for instance Hochet, Dodet, Ardhuin, Hemer, and Young (2021)) and downloaded from the NOAA website (Hurrell & Staff, 2020). All indices except NINO3.4 are based on Empirical Orthogonal functions of SLP. NINO3.4 is obtained from SST average in a region of the tropical Pacific (see (Hurrell & Staff, 2020)). Only 5 % significant correlations are shown.

References

Bricheno, L. M., & Wolf, J. (2018). Future wave conditions of europe, in response to high-end climate change scenarios. *Journal of Geophysical Research: Oceans*, *123*(12), 8762–8791.

Erikson, L., Morim, J., Hemer, M., Young, I., Wang, X., Mentaschi, L., ... others (2022). Global ocean wave fields show consistent regional trends between 1980 and 2014 in

a multi-product ensemble. *Communications Earth & Environment*, *3*(1), 320.

Hersbach, H., Bell, B., Berrisford, P., Hirahara, S., Horányi, A., Muñoz-Sabater, J., ... Thépaut, J.-N. (2020). The ERA5 global reanalysis. *Quarterly Journal of the Royal Meteorological Society*, *146*(730), 1999–2049. Retrieved 2020-08-26, from https://rmets.onlinelibrary.wiley.com/doi/abs/10.1002/qj.3803 (_eprint: https://rmets.onlinelibrary.wiley.com/doi/pdf/10.1002/qj.3803) doi: 10.1002/qj.3803

Hochet, A., Dodet, G., Ardhuin, F., Hemer, M. A., & Young, I. (2021). Sea state decadal variability in the north atlantic: a review. , ?

Hurrell, J., & Staff, N. (2020). *The climate data guide: Hurrell north atlantic oscillation (nao) index (station-based).* https://climatedataguide.ucar.edu/climate-data/hurrell-north-atlantic-oscillation-nao-index-station-based. (Last modified 24 Apr 2020.)

Mentaschi, L., Vousdoukas, M. I., Voukouvalas, E., Dosio, A., & Feyen, L. (2017). Global changes of extreme coastal wave energy fluxes triggered by intensified teleconnection patterns. *Geophysical Research Letters*, *44*(5), 2416–2426.

Reguero, B., Menéndez, M., Méndez, F., Mínguez, R., & Losada, I. (2012). A global ocean wave (gow) calibrated reanalysis from 1948 onwards. *Coastal Engineering*, *65*, 38–55.

Sharmar, V. D., Markina, M. Y., & Gulev, S. K. (2021). Global ocean wind-wave model hindcasts forced by different reanalyzes: A comparative assessment. *Journal of Geophysical Research: Oceans*, *126*(1), e2020JC016710.

Retrieved from https://agupubs.onlinelibrary.wiley.com/doi/abs/10.1029/2020JC016710 (e2020JC016710 2020JC016710) doi: https://doi.org/10.1029/2020JC016710

Smith, G. A., Hemer, M., Greenslade, D., Trenham, C., Zieger, S., & Durrant, T. (2021). Global wave hindcast with australian and pacific island focus: From past to present. *Geoscience Data Journal*, *8*(1), 24-33. Retrieved from https://rmets.onlinelibrary.wiley.com/doi/abs/10.1002/gdj3.104 doi: https://doi.org/10.1002/gdj3.104

Stopa, J. E., Ardhuin, F., Babanin, A., & Zieger, S. (2016). Comparison and validation of physical wave parameterizations in spectral wave models. *Ocean Modelling*, *103*, 2–17.

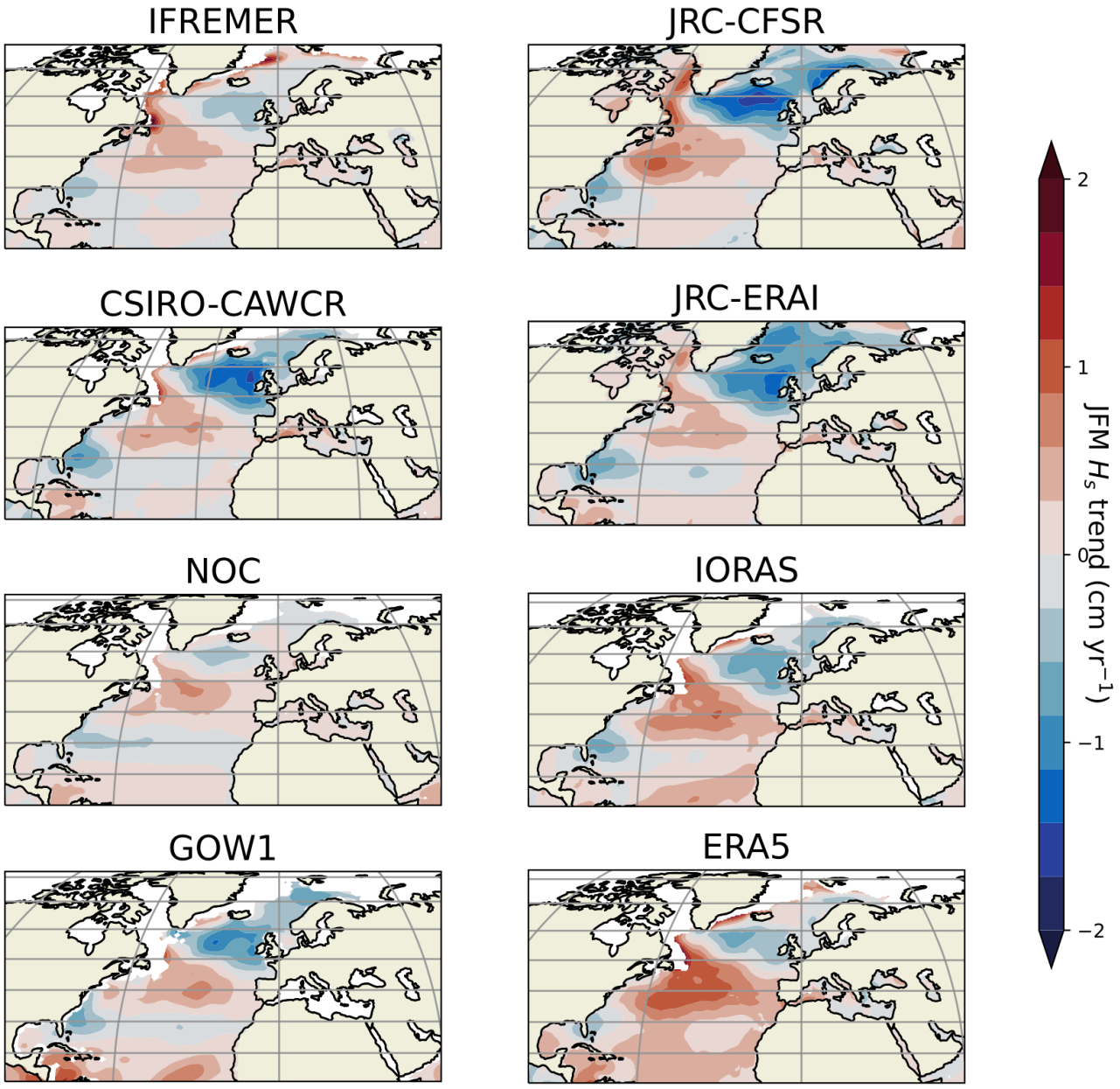

Figure S1. Comparison of the 1980-2014 JFM H_s trends in the North Atlantic for 8 different datasets.

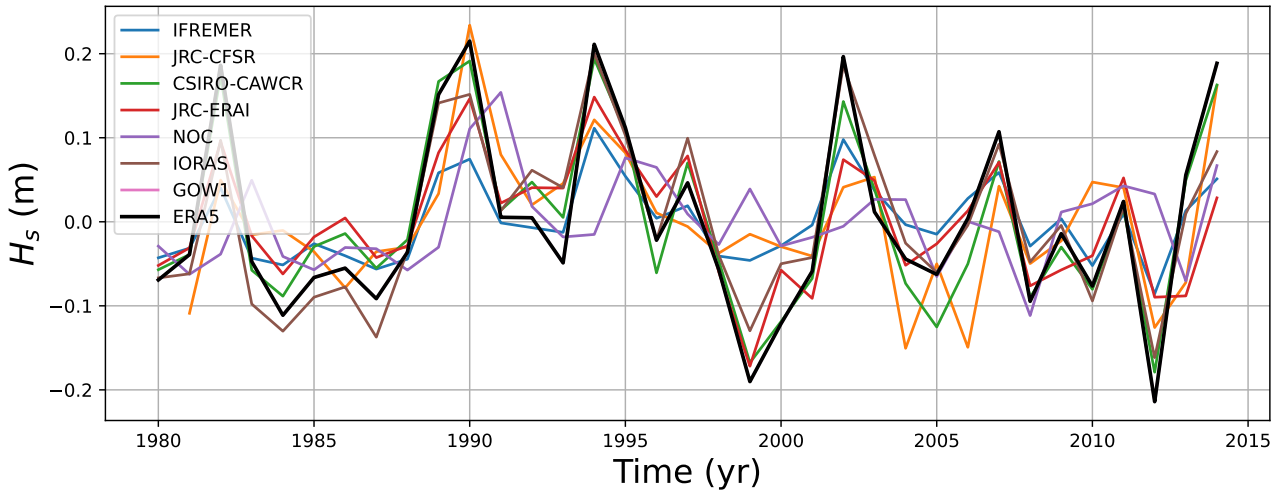

Figure S2. Time series of the NA average JFM H_s anomalies obtained from 8 different dataset. The ERA-5 time serie, used in this article, is shown in black.

Table S1. Time correlation between the JFM average of the main North Atlantic climate indices and H_s in the three locations. Only 5 % significant correlations are shown. The considered indices are: the North Atlantic Oscillation (NAO), the Eastern Atlantic pattern (EA), the Scandinavian index (SCAN), the Eastern Atlantic Western Russia index (EAWR), the Pacific North America index (PNA), the NINO3.4 index (el nino) and the Tropical Northern Hemisphere index (TNH).

	NAO	EA	SCAN	EAWR	PNA	el nino	TNH
Norwegian Sea	0.66		-0.55	-0.28			
Western Mediterranean Sea	-0.29	-0.42		-0.29			
U.S. East Coast	-0.65					0.26	

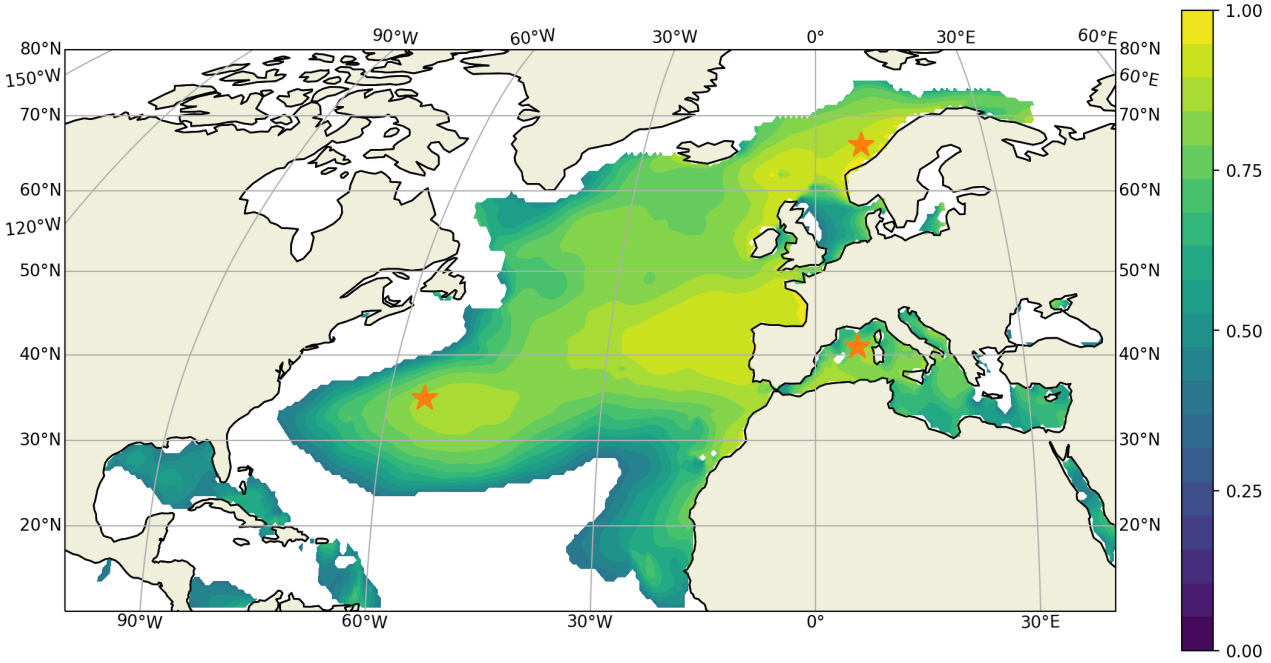

Figure S3. Time correlation between the 1993-2018 reconstructed H_s and ERA-5 H_s. Only 5% significant values are shown. The three specifically studied locations are indicated with orange stars.

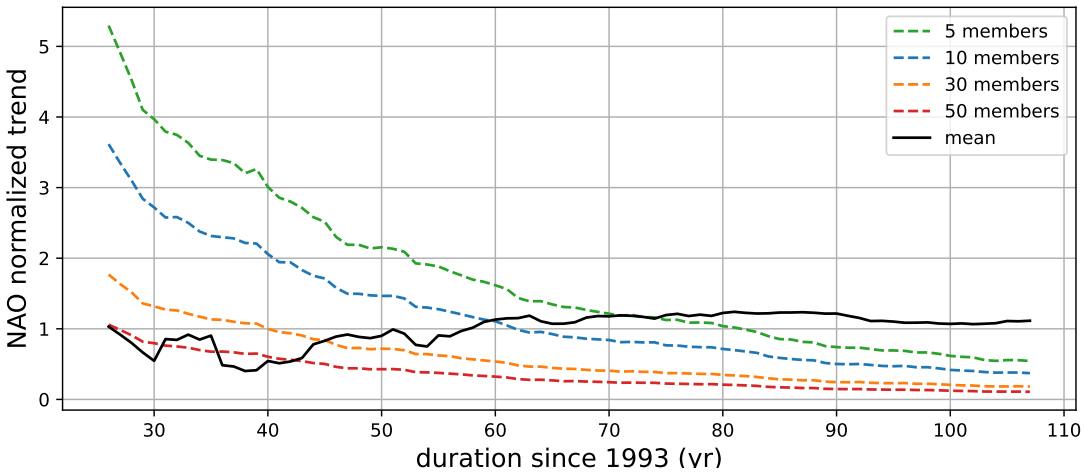

Figure S4. Ensemble mean trend of the North Atlantic Oscillation index (black line) and 1.64 standard deviation of the same index (dashed) computed using 5, 10, 30 and 50 members of the CESM2 LENS2 ensemble. The trends are given as a function of the duration since 1993 (in year). The date (or duration) for which the 1.64 standard deviation curve for X members (X=5, 10, 30 or 50) intersects the ensemble mean (black) curve can be interpreted as the date of emergence of the forced signal in the X-member sub-ensemble. The forced NAO trend can be extracted with only 5 members if we consider trends longer than 70 years, whereas more than 50 members are required for trends shorter than 30 years.

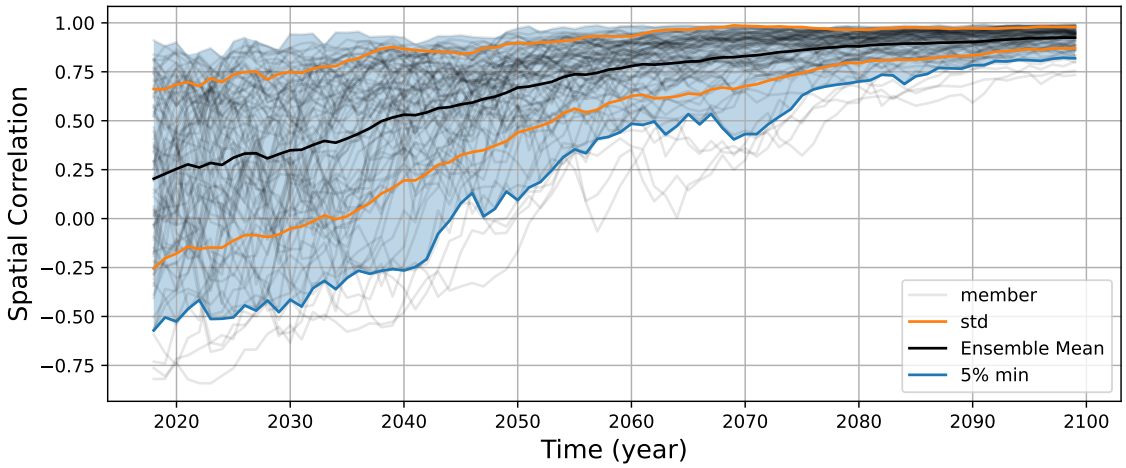

Figure S5. Spatial correlation between the H_s trend computed on the ensemble mean and the trend computed on each individual members between 1993 (the CCI v1 dataset start) and the end date shown as the x-coordinate. The black line is the mean of the spatial correlation between the ensemble mean trend and each individual member trend, the orange lines show the values that are within one standard deviation from the mean, blue shading shows members with 95% of the largest correlation values and the blue line is the separation between the 5% smallest values and 95% largest.